

NASA Technical Memorandum 88799

# Diffusion Flame Extinction in Slow Convective Flow Under Microgravity Environment

(NASA-TM-88799) DIFFUSION FLAME EXTINCTION  
IN SLOW CONVECTIVE FLOW UNDER MICROGRAVITY  
ENVIRONMENT (NASA) 16 p HC A02/MF A01  
CSCL 20D

N86-28378

G3/34      **Unclas**  
43494

Chiun-Hsun Chen  
*Lewis Research Center*  
*Cleveland, Ohio*

Prepared for the  
Microgravity Fluid Mechanics Symposium  
sponsored by the American Society of Mechanical Engineers  
Anaheim, California, December 10-11, 1986

**NASA**

DIFFUSION FLAME EXTINCTION IN SLOW CONVECTIVE FLOW UNDER MICROGRAVITY ENVIRONMENT

Chiun-Hsun Chen\*  
National Aeronautics and Space Administration  
Lewis Research Center  
Cleveland, Ohio 44135

ABSTRACT

A theoretical analysis is presented to study the extinction characteristics of a diffusion flame near the leading edge of a thin fuel plate in slow, forced convective flows in a microgravity environment. The mathematical model includes two-dimensional Navier-Stokes momentum, energy and species equations with one-step overall chemical reaction using second-order finite rate Arrhenius kinetics. Radiant heat loss on the fuel plate is applied in the model as it is the dominant mechanism for flame extinguishment in the small convective flow regime. A parametric study based on the variation of convective flow velocity, which varies the Damkohler number (Da), and the surface radiant heat loss parameter (S) simultaneously, is given. An extinction limit is found in the regime of slow convective flow when the rate of radiant heat loss from fuel surface outweighs the rate of heat generation due to combustion. The transition from existent envelope flame to extinguishment consists of gradual flame contraction in the opposed flow direction together with flame temperature reduction as the convective flow velocity decreases continuously until the extinction limit is reached. A case of flame structure subjected to surface radiant heat loss is also presented and discussed.

NOMENCLATURE

As pre-exponential factor for fuel pyrolysis,  $A\bar{S}/\rho^*$   
 $\bar{B}$  dimensional frequency factor for gas phase reaction,  $[m^3 \cdot kg^{-1} \cdot s^{-1}]$   
 $\bar{c}_p$  average specific heat  $[kJ \cdot kg^{-1} \cdot k^{-1}]$   
 $\bar{D}$  dimensional species diffusivity  $[m^2 \cdot s^{-1}]$   
 Da Damkohler number,  $(k^*/\bar{c}_p u_\infty^2) \bar{B}$

E activation energy for gas phase reaction,  $\bar{E}/RT_\infty$   
 Es activation energy for fuel pyrolysis,  $\bar{E}_s/RT_\infty$   
 f stoichiometric oxidizer/fuel mass ratio  
 $k^*$  thermal conductivity at  $T^*$   $[W \cdot m^{-1}k^{-1}]$   
 L latent heat,  $\bar{L}/c_p T_\infty$   
 Le Lewis number,  $\bar{\alpha}/\bar{D}$   
 $\dot{m}$  blowing rate on the fuel plate,  $\bar{m}/\rho^* u_\infty$   
 Pr Prandtl number,  $\bar{\nu}/\bar{\alpha}$   
 p pressure,  $(\bar{p} - \bar{p}_{rc})/\rho^* u_\infty^2$   
 $\bar{p}_{rc}$  absolute pressure at arbitrary reference point [Pa]  
 Q heat of reaction per unit mass of fuel,  $\bar{Q}/\bar{c}_p T_\infty$   
 $\dot{Q}$  rate of heat generation per unit volume,  $Q\dot{\omega}_f$   
 R universal gas constant  $[kg \cdot m^2 \cdot s^{-2} \cdot kg^{-1} \cdot mole^{-1} \cdot k^{-1}]$   
 Re Reynolds number,  $\rho^* u_\infty \delta / u^*$   
 r ratio of reference temperature to ambient temperature,  $T^*/T_\infty$   
 S surface radiant heat loss parameter,  $\epsilon \sigma T_\infty^3 / \rho^* \bar{c}_p u_\infty$   
 $T^*$  reference temperature [K]  
 T temperature,  $\bar{T}/T_\infty$   
 $T_s$  pyrolysis temperature,  $\bar{T}_s/T_\infty$   
 $T_w$  fuel surface temperature,  $\bar{T}_w/T_\infty$   
 $T_\infty$  ambient temperature [k]

E-3137

\*National Research Council - NASA Research Associate.

$u$  velocity parallel to fuel surface,  $\bar{u}/u_\infty$   
 $u_\infty$  free stream velocity,  $[m \cdot s^{-1}]$   
 $v$  velocity normal to fuel surface,  $\bar{v}/u_\infty$   
 $x$  distance along fuel surface,  $\bar{x}/\delta$   
 $x_{max}$  location of upstream boundary  
 $x_{min}$  location of downstream boundary  
 $Y_F$  mass fraction of fuel,  $\bar{\rho}_F/\bar{\rho}$   
 $Y_{F\infty}$  ambient fuel mass fraction  
 $Y_O$  mass fraction of oxidizer,  $\bar{\rho}_O/\bar{\rho}$   
 $Y_{O\infty}$  ambient oxidizer mass fraction  
 $y$  distance normal to fuel surface,  $\bar{y}/\delta$   
 $y_{max}$  location of free stream boundary  
 $\alpha^*$  thermal diffusivity at  $T^*$ ,  $[m^2 \cdot s^{-1}]$   
 $\delta$  thermal distance,  $\alpha^*/u_\infty$ ,  $[m]$   
 $\epsilon$  total hemispherical emissivity of the fuel surface  
 $\mu^*$  dynamic viscosity at  $T^*$ ,  $[kg \cdot m^{-1} \cdot s^{-1}]$   
 $\mu$  dynamic viscosity,  $\bar{\mu}/\mu^*$   
 $\rho^*$  density at  $T^*$ ,  $[kg \cdot m^{-3}]$   
 $\rho$  density,  $\bar{\rho}/\rho^*$   
 $\sigma$  Stefan-Boltzman constant  $[W \cdot m^{-2} \cdot K^{-4}]$   
 $\omega_F$  nondimensional fuel reactivity,  $-Da\rho^2 Y_F Y_O \exp(-E/T)$

#### Overhead

- dimensional quantities

#### Superscript

\* reference state

#### Subscript

$F$  fuel  
 $O$  oxidizer  
 $w$  surface of fuel plate  
 $\infty$  ambient  
 $max$  maximum  
 $min$  minimum

#### INTRODUCTION

The study is concerned with the extinction mechanism of diffusion flame adjacent to a thin fuel plate in slow convective flow as shown in Fig. 1. The major application for this class of problem is fire safety in manned spacecraft and space station where the

gravity effect is negligible. Under these circumstances, natural convection is neglected. But a forced flow can exist due to the air ventilation in the living quarters of the astronauts. This convective velocity can be small, less than the natural-convective velocity around the flame in earth environment which is of the order of 15 cm/s. With the increasing concern of fire safety in spacecraft and accelerated experimental efforts to test the flammability characteristics of solid materials in microgravity at NASA Lewis Research Center, this effort describes the theoretical investigation coordinated with experimental task.

The present analysis is an extension of earlier work (1). In that work, the blowoff phenomena for a two-dimensional diffusion flame around the leading edge of a thin fuel plate were investigated. The primary parameter varied in the computation is the Damkohler number,  $Da$ , defined as  $(\rho^* \alpha^* / u_\infty^2) B$  where  $\rho^*$  and  $\alpha^*$  are density and thermal diffusivity of the gas in reference state respectively,  $u_\infty$  is the convective flow velocity and  $B$  is the frequency factor of chemical reaction. Lowering  $Da$  corresponds to increasing  $u_\infty$  for a given fuel. The blowoff phenomena predicted by the previous theoretical model (1) is what we observe in ordinary experience. However, the velocity range of interest in microgravity application is when  $u_\infty$  becomes small. In Ref. 1, only one nondimensional parameter contains  $u_\infty$ , i.e., the Damkohler number. When  $u_\infty \rightarrow 0$ ,  $Da \rightarrow \infty$  which according to (1) is moving away from blowoff or extinction. At the same time, it is also found that dimensionally the fuel burning rate is very small and the flame stand-off distance is large. In other words, in the limit of small convective flow velocity, a kinetically-strong (large  $Da$ ), large size but low power (small burning rate) flame exists. This conclusion is a contradiction to the experimental observations (2,3) which show lower flame temperature and flame spreading rate in zero-g condition. It implies that certain key elements may be missing in the model for small convective flow regime. The missing link appears to be the radiant heat loss which becomes important for a flame with small heat release rate due to reduced oxidizer supply rate. In this case, heat loss owing to radiation can be the dominant mechanism for flame extinction.

Bonne (4), to the author's best knowledge, is the first one to investigate the influence of radiative heat transfer on diffusion flame under zero-g environment. From both experimental work and theoretical analysis by using a flat diffusion flame, he concludes that the radiant heat loss results in the reduction of flame temperature which leads to extinguishment. Recently, T'ien (5) imposed a radiative heat loss term into the energy balance on the condensed fuel surface for a stagnation-point diffusion flame. Without the effect of gravity, he identifies a new extinction branch at the regime of sufficiently small flame stretch rate and also finds the radiative contribution to extinction is through the reduction of flame temperature.

In the other studies the primary purposes may not be microgravity combustion research, but they can give the important indication of the role of radiation in contributing to flame extinction. Sibulkin, Kulkarni and Annamalai (6) analyze the radiative effects on the laminar, natural-convective burning of a thermally thick, vertical fuel surface by a use of local similarity approximation. The results show that gas phase radiation has a negligible effect on burning rate, however, heat losses due to surface radiation are a sufficient condition for extinction even in the limit

**ORIGINAL PAGE IS  
OF POOR QUALITY**

of infinite-fast chemical reaction. In Ref. 7, Sohrab, Linan and Williams applied asymptotic technique to investigate the diffusion flame with gaseous radiant heat loss in a stagnation-point boundary layer geometry. Another work by Sohrab and Williams (8) studied the diffusion flames adjacent to flat, condensed fuels with surface radiation heat loss. In both papers, the authors find that the diffusion flames in the stagnation-point flow can be extinguished by providing additional radiant losses from the gas phase or on the fuel surface which will decrease the available enthalpy of combustion of the fuel, thereby lowering the flame temperature.

The specific problem to be treated in this study is to apply the radiative heat loss on the fuel surface to the combustion model of Ref. 1. With the additional heat loss term in the energy balance, the burning rate of the fuel is expressed by an Arrhenius-type pyrolysis law. Also it is assumed that the flow is steady, laminar and two-dimensional, and no burnout of fuel sample is included. Radiative heat transfer in the gas phase is not considered here.

**MATHEMATICAL MODEL**

Except for the modified boundary conditions, such as the radiant heat loss in the energy balance and the pyrolysis expression applied on the fuel surface, the present combustion model is the same as that in Ref. 1. The governing system is elliptic in nature which includes conservation equations for mass, momentum, energy and species in differential form. An equation of state and the variation of viscosity with temperature are used as the linkages between properties. An assumed chemical reaction rate is also included in this system. Finally, a set of known boundary conditions is specified to complete the mathematical description of the problem.

The nondimensional governing equations and boundary conditions, with the coordination defined in Fig. 1, are as follows.

**Governing Equations:**

**Continuity equation:**

$$\frac{\partial(\rho u)}{\partial x} + \frac{\partial(\rho v)}{\partial y} = 0 \quad (1)$$

**Momentum equations:**

$$\rho u \frac{\partial u}{\partial x} + \rho v \frac{\partial u}{\partial y} = -\frac{\partial p}{\partial x} + \frac{\mu}{\text{Re}} \left\{ 2 \frac{\partial^2 u}{\partial x^2} - \frac{2}{3} \left( \frac{\partial u}{\partial x} + \frac{\partial v}{\partial y} \right) \right\} + \frac{\mu}{\text{Re}} \left[ \frac{\partial}{\partial y} \left( \frac{\partial u}{\partial y} + \frac{\partial v}{\partial x} \right) \right] \quad (2)$$

$$\rho u \frac{\partial v}{\partial x} + \rho v \frac{\partial v}{\partial y} = -\frac{\partial p}{\partial y} + \frac{\mu}{\text{Re}} \left[ \frac{\partial}{\partial x} \left( \frac{\partial u}{\partial y} + \frac{\partial v}{\partial x} \right) \right] + \frac{\mu}{\text{Re}} \left\{ 2 \frac{\partial^2 v}{\partial y^2} - \frac{2}{3} \left( \frac{\partial u}{\partial x} + \frac{\partial v}{\partial y} \right) \right\} \quad (3)$$

**Energy equation:**

$$\rho u \frac{\partial T}{\partial x} + \rho v \frac{\partial T}{\partial y} = \frac{1}{\text{RePr}} \left[ \frac{\partial}{\partial x} \left( \mu \frac{\partial T}{\partial x} \right) + \frac{\partial}{\partial y} \left( \mu \frac{\partial T}{\partial y} \right) \right] + \dot{Q}_F \quad (4)$$

**Fuel species equation:**

$$\rho u \frac{\partial Y_F}{\partial x} + \rho v \frac{\partial Y_F}{\partial y} = \frac{1}{\text{RePrLe}} \left[ \frac{\partial}{\partial x} \left( \mu \frac{\partial Y_F}{\partial x} \right) + \frac{\partial}{\partial y} \left( \mu \frac{\partial Y_F}{\partial y} \right) \right] + \dot{\omega}_F \quad (5)$$

**Oxidizer species equation:**

$$\rho u \frac{\partial Y_O}{\partial x} + \rho v \frac{\partial Y_O}{\partial y} = \frac{1}{\text{RePrLe}} \left[ \frac{\partial}{\partial x} \left( \mu \frac{\partial Y_O}{\partial x} \right) + \frac{\partial}{\partial y} \left( \mu \frac{\partial Y_O}{\partial y} \right) \right] + \dot{\omega}_F \quad (6)$$

where

$$\dot{\omega}_F = -\text{Da} \rho^2 Y_F Y_O \text{EXP}(-E/T) \quad (7)$$

is the nondimensional fuel reaction rate for which the definition of Da can be found later in Eq. (16).

**Equation state:**

$$\rho T = \frac{T^*}{r} = r \quad (8)$$

where r is the ratio of reference temperature to the ambient one (see Ref. 1).

The viscosity variation with temperature is taken to be

$$\mu = \frac{1}{r} T \quad (9)$$

**Boundary conditions:**

At  $x = x_{\min}$

$$u = 1, v = 0, T = 1, Y_F = 0, Y_O = Y_{O\infty} \quad (10)$$

At  $x = x_{\max}$

$$\frac{\partial u}{\partial x} = \frac{\partial v}{\partial x} = \frac{\partial T}{\partial x} = \frac{\partial Y_F}{\partial x} = \frac{\partial Y_O}{\partial x} = 0 \quad (11)$$

At  $y = y_{\max}$

$$u = 1, \frac{\partial v}{\partial y} = 0, T = 1, Y_F = 0, Y_O = Y_{O\infty} \quad (12)$$

At  $y = 0$

for  $x_{\min} \leq x < 0$

$$\frac{\partial u}{\partial y} = 0, v = 0, \frac{\partial T}{\partial y} = 0, \frac{\partial Y_F}{\partial y} = 0, \frac{\partial Y_O}{\partial y} = 0 \quad (13)$$

for  $0 \leq x \leq x_{\max}$

$$u = 0, \dot{m}_w = \rho_w v_w = A_s \text{EXP}(-E_s/T_s), T_w = T_s$$

$$\dot{m}_{Fw} = \dot{m} + \frac{1}{\text{RePrLe}} \frac{\partial Y_F}{\partial y} \Big|_w \quad (14)$$

$$\dot{m}_{Ow} = \frac{1}{\text{RePrLe}} \frac{\partial Y_O}{\partial y} \Big|_w$$

$$\frac{\mu}{\text{RePr}} \frac{\partial T}{\partial y} \Big|_w = \dot{m} L + S(T_s^4 - 1)$$

where  $A_s$  and  $E_s$  are a pre-exponential factor and activation energy for surface pyrolysis respectively.

$S$  is the surface radiant heat loss parameter; defined as

$$S = \frac{\epsilon \sigma T_{\infty}^3}{\rho^* C_p u_{\infty}} \quad (15)$$

where  $\epsilon$  is the total hemispherical emissivity of the fuel surface and  $\sigma$  is the Stefan-Boltzman constant.

From above definition,  $S$  is a function of  $u_{\infty}$  if  $\epsilon \neq 0$ . Another parameter in this study which also contains  $u_{\infty}$  is the Damkohler number, shown in Eq. (7), expressed as

$$Da = \left( \frac{k^*}{C_p u_{\infty}^2} \right) \bar{g} \quad (16)$$

For a given fuel under specified ambient condition, changing the convective flow velocity ( $u_{\infty}$ ) will change both  $Da$  and  $S$  (see Eqs. (15) and (16)). Eventually, large  $Da$  implies a kinetically-strong flame in the gas phase. On the other hand, large  $S$  implies large heat loss to the fuel plate. So the resultant flame structure apparently depends on the competition between  $Da$  and  $S$ .

One important feature of the boundary conditions at the fuel surface needs to be mentioned. Because of the use of Arrhenius pyrolysis law for the fuel, the temperature distribution along the wall is no longer prescribed as in Ref. 1, but provided as a result of the calculation.

The normalization procedure for these equations is described in Ref. 1. The problem is solved numerically. The computer code using the SIMPLE procedure (9) is developed and modified by the author. The algorithm is vectorized in order to utilize the performance of the supercomputer CRAY-1/S at Lewis.

## RESULTS and DISCUSSIONS

There are 13 parameters in this study which are derived from the normalization procedure through the governing system. Their composite groups of physical properties and quantities are shown in Table I. The values of these properties are the same as that used in Ref. 1. As to the additional properties, such as  $A_s$  and  $E_s$ , their values are adopted from Ref. 5. Only the effect of a variable convective flow velocity ( $u_{\infty}$ ), which changes  $Da$  and  $S$  simultaneously, is investigated with and without radiant heat loss ( $\epsilon = 1$  and  $\epsilon = 0$ ). According to the variation of the flow velocity in the regime of interest ( $< 20$  cm/s), the computation is categorized into 8 cases which are listed in Table II.

For  $\epsilon = 0$  which implies no surface radiant heat loss is involved, the results confirm that the similarity relationship still exists at large  $Da$  as found in Ref. 1, even though the surface boundary conditions for both studies are different. Figure 2(a) shows the temperature contour distributions for  $Da$  ranging from  $2.81 \times 10^6$  to  $7.20 \times 10^8$ . For this range of  $Da$  envelope flames exist in the gas phase ahead of the leading edge ( $x = y = 0$ ) of the fuel plate. Except for a very narrow region of high temperature, for example  $T > 6.9$  (which are not shown in this figure), the temperature distributions are found to be nearly invariant with  $Da$  in the regime of small convective flow velocity.

In Fig. 3 the maximum flame temperature ( $T_{max}$ ) is plotted against the Damkohler number ( $Da$ ). For  $\epsilon = 0$ , the  $T_{max}$  in gas phase is increasing with  $Da$

but the magnitude of temperature rise is very slight compared to the increment of  $Da$ . It indicates that the larger  $Da$  is, the more kinetically-strong the flame becomes, even though physically the fuel supply rate is smaller. Figure 4 is temperature distribution along the fuel surface which is directly related to the fuel evaporation rate (see Eq. (14)). As before, the wall temperature profiles are found to be indistinguishable from one another for a wide range of  $Da$  under the condition  $\epsilon = 0$ . From the above description, the essential characteristics of the flame without radiant heat loss in the slow convective flow regime are similar to those obtained in Ref. 1. That is, envelope diffusion flames exist at large  $Da$  where the computed fuel evaporation rate, the flame stand-off distance and velocity profiles show certain similitude.

However, the similarity relationship breaks down and the flame is quenched at a large  $Da$  ( $7.20 \times 10^8$ ) when the condition  $\epsilon = 1$ , corresponding to the black-body surface radiation, is applied. The isotherm distributions of the flame as a function of flow velocity ( $u_{\infty}$ ) are illustrated in Figs. 2(b) to (h). The transition from a strong flame to extinction consists of a series of flame contractions. The flame fronts are found to maintain their positions ahead of the leading edge of the fuel plate and the flame quench trend by radiation is proceeding in the opposed flow direction during the transition. Comparing Fig. 2(a) (without surface radiation) with Figs. 2(b) and (c) we see that the flames shift toward the fuel plate in the  $y$ -direction but show little variations in  $x$ -direction. As  $u_{\infty}$  becomes smaller, as in the Fig. 2(d), the flame appears to be shortening in the  $x$ -direction. We start to see the complete isotherms  $T = 5$  and  $T = 6$  in the gas phase and the isotherm  $T = 4$  intends to form the closing end. In other words, the fire plume, where the fuel surface stops pyrolyzing, appears in the downstream gas phase. The flame size keeps shrinking as  $u_{\infty}$  continues to decrease. Now, we can see the close-ended isotherms  $T = 4$  in Fig. 2(e) and  $T = 3$  in Fig. 2(f). Finally, the isotherm  $T = 6$  disappears in the vicinity of leading edge zone (flame stabilization zone) in Fig. 2(h). And from Case 3s, it becomes clear that the flame contraction is more significant in streamwise direction than that in cross-stream direction. For instance, the displacement in  $x$ -direction for the flame tip of isotherm  $T = 5$  is about 40 thermal lengths from Figs. 2(d) to 2(h), but it is less than 10 thermal distances in  $y$ -direction. As soon as  $u_{\infty}$  reaches a critical value ( $= 1.25$  cm/s), the flame no longer exists; radiant flame extinguishment occurs.

Another characteristic of the transition to extinction can also be seen in Figs. 3 and 4. Figure 3 shows  $T_{max}$  decreasing instead of increasing as  $u_{\infty}$  decreases (or  $Da$  increases) when the surface radiant heat loss is imposed. Near the extinction limit, the rate of flame temperature decay becomes even more dramatic. From the physical point of view, we have a low-power flame when the fuel supply rate is reduced. Figure 4 shows the temperature profiles along the fuel surface which are coupled to the thermal structures in gas phase. For the convenience of the study, the end of the fuel pyrolysis is designated as soon as  $V_w$  (blowing velocity) is less than 0.001 where the correspondent wall temperature is 1.70. Since the flame front is stabilized at the leading edge during the transition (see Fig. 2), the maximum surface temperature and blowing velocity are expected there. In the cases of 1s and 2s, because the flames cover the full range of the fuel plate  $x \leq 50$ , the downstream temperature profiles

behind the leading edge are more or less similar to the ones without radiation ( $\epsilon = 0$ ) but with lower magnitudes. From Case 3s, the fire plume starts to appear within the domain of interest. As  $u_w$  becomes smaller, the pyrolysis length becomes shorter which implies that the fuel supply rate is lower and the flame is weaker.

Figures 2 to 4 together provide the complete picture for radiant flame extinguishment. The author mentioned earlier that the flame structure depends on the interaction between  $Da$  and  $S$ . From the implication of similarity in Figs. 2(a) and 4, increasing  $Da$  does not affect the fuel evaporation rate as long as the Damkohler number is greater than  $2.81 \times 10^6$ . Even the maximum flame temperature rises very little from  $Da = 2.81 \times 10^6$  to  $Da = 2.71 \times 10^8$  as shown in Fig. 3. It indicates the heat generation rate from combustion approaches an asymptotic value at large  $Da$ . As  $S$  increases with  $Da$ , the heat loss rate to the fuel plate becomes proportionally greater in significance than that of heat generation. In other words, at the regime of slow convective flow, the radiant heat loss from the fuel surface becomes so great that the available energy from gas phase to pyrolyze the fuel is greatly reduced. The fuel supply rate is thus reduced. As a consequence, the gas phase heat release rate is lowered, thereby the flame temperature is decreased, the flame size is contracted and the pyrolysis length is shortened.

The large  $Da$  contributes to stabilizing the flame front ahead of the leading edge by providing the opportunity for fuel vapor to diffuse upstream into the flame. Since the flame front consumes a large portion of the limited amount of fuel vapor due to the shortened pyrolysis length, the extension of combustion to the downstream is delimited and the finite rate kinetics effect becomes crucial. Therefore the flame is quenched downstream and the flame contraction moves upstream during the transition. Finally, the flame disappears in the stabilization zone.

Although the surface radiation is emphasized as the dominant factor for flame extinction in this study, its influence is coupled with the finite-rate reaction in the gas phase where the streamwise heat conduction and mass diffusion are responsible for flame stabilization around the leading edge and the downstream existence of the fire plume. Therefore the transition to extinction exhibits multi-dimensional behavior.

Next, Case 4s is chosen to study the flame structure within the transition. The temperature contour has been shown in Fig. 2(e). The flame front is situated ahead of the leading edge of the fuel plate. However, the flame does not continue downstream where a fire plume region exists. This can be seen clearly in Fig. 5 which is the fuel reactivity contour distribution ( $-\dot{\omega}_F$ ; see Eq. (7) for definition). The most reactive zone occurs in the flame front such that it can stabilize the flame in front of the leading edge. In the downstream region, the reaction cannot be sustained but is frozen in the gas phase due to the lack of fuel supply. Figure 6 gives the mass fraction distributions for fuel and oxidizer for this case. Since the most vigorous reaction zone is located at the flame front, a strong mass diffusion is required in streamwise direction to drive the fuel vapor upstream in order to maintain the reaction ahead of the leading edge. The short pyrolysis length (only about 10 thermal distances, see fig. 4) results in a reduced fuel supply which is indicated by the attachment of  $Y_F = 0.01$  fuel contour to the fuel plate. The oxidizer contour is shifted toward the fuel plate much further downstream.

Figures 7 and 8 are relative isobar contours and the velocity vector field respectively. There are two pressure plateaus existing in the flow field. One is at the flame front, caused by the hot product gas thermal expansion, which retards/deflects the flow ahead of it and accelerates the flow behind it. The other pressure plateau is due to the existence of the stagnation point. With the dual effects of the stagnant pressure and the shear stress induced by the vertical blowing velocity, the flow is strongly deflected near the leading edge. Far from the fuel plate, the flow is not disturbed since the flame is small. In the downstream region, the reaction is complete and the flow is parallel to the fuel plate.

The author is not yet aware of any experimental work or theoretical investigation which has the same model and flow configuration as the present study. Therefore comparisons with other works are based on the limited similarities which can be shown.

The theoretical study by Sibulkin et al. (6) has the same solid fuel geometry as the present one but the flow is naturally-induced and is analyzed by the use of local similarity approximation. In that paper the authors show that surface radiation heat loss can result in extinction. However, the radiation is treated without any physical connection to the other factors as in the present study. Also by neglecting the streamwise effects due to the application of local similarity, the flame extinction is a local phenomenon which is quite different from the basic emphasis of this study that the flame extinguishment is a multi-dimensional phenomenon.

That flame temperature is reduced because of the inclusion of radiation is universally recognized in these works by Bonne (4), T'ien (5), Sibulkin et al. (6), Sohrab et al. (7) as well as Sohrab and Williams (8). The reactivity distribution in fire plume region resembles the profiles described in Chen and T'ien's work (10) which studies the effects of the finite rate chemical kinetics in the fire plume. The retardation/deflection of flow in front of the flame and the flow acceleration behind the flame are observed experimentally by Hirano and Kinoshita (11). All of the Navier-Stokes calculation allowing the thermal expansion, such as Lee and T'ien (12), Mao et al. (13) and Ref. 1, reproduce the phenomena. Although the flow configuration is in stagnation-point geometry, T'ien (5) confirms a radiant extinguishment branch at small flame stretch rates where in this study the flame is quenched in the regime of slow convective flow velocity.

## CONCLUSION

A model of a diffusion flame at the leading edge of a fuel plate in slow, forced convective flow under zero-g environment has been developed and solved numerically to study the flame extinguishment phenomena. The extinction mechanism in the small velocity regime is different from that of blowoff, and radiative heat loss is the dominant factor. The mathematical system consists of two-dimensional Navier-Stokes momentum, energy and species equations. A one-step overall chemical reaction with second-order finite-rate Arrhenius kinetics is also included. Radiant heat loss on the fuel surface is applied to the combustion model as well as an application of an Arrhenius-type surface pyrolysis law.

After the nondimensionalization procedure, two essential parameters are specified. These are the Damkohler number ( $Da$ ) and the surface radiant heat loss parameter ( $S$ ) respectively. For given fuel and

ambient conditions, the effect of a variable convective flow velocity, which changes  $Da$  and  $S$  simultaneously, is investigated.

An extinction limit is identified at the small velocity regime. From existent envelope flame to flame extinguishment, the flame front is found to maintain itself ahead of the leading edge of the fuel plate. The transition, which is a multidimensional phenomenon, consists of a series of flame contractions and pyrolysis length reductions in the opposed flow direction as well as a flame temperature depression. As the convective flow velocity is lowered to a limiting value, the radiant heat loss rate sufficiently outweighs the heat generation rate and the radiant flame extinguishment occurs.

#### REFERENCES

1. Chen, C.H. and T'ien J.S., "Diffusion Flame Stabilization at the Leading Edge of a Fuel Plate," to be published in Combustion Science and Technology, 1986.
2. Andracchio, C.R. and Aydelott, J.C., "Comparison of Flame Spreading Over Thin Flat Surfaces in Normal Gravity and Weightlessness in an Oxygen Environment," NASA TM X-1992, 1970.
3. Cochran, T.H. Petrash, D.A., Andracchio, C.R. and Sotos, R.G., "Burning of Teflon-Insulated Wires in Supercritical Oxygen at Normal and Zero Gravities," NASA TM X-2174, 1971.
4. Bonne, U. "Radiative Extinguishment of Diffusion Flames at Zero Gravity," Combustion and Flame, Vol. 16, No. 2, Apr. 1971, pp. 147-159.
5. T'ien, J.S., "Diffusion Flame Extinction at Small Stretch Rates: The Mechanism of Radiative Loss," Combustion and Flame, Vol. 65, No. 1, July 1986, pp. 31-34.
6. Sibulkin M., Kulkarni, A.K. and Annamalai, K., "Effects of Radiation on the Burning of Vertical Fuel Surfaces," Eighteenth Symposium (International) on Combustion, The Combustion Institute, Pittsburgh, 1981, pp. 611-617.
7. Sohrab, S.H., Linan, A. and Williams, F.A., "Asymptotic Theory of Diffusion-Flame Extinction with Radiant Loss from the Flame Zone," Combustion Science and Technology, Vol. 27, No. 3 and 4, 1982, pp. 143-154.
8. Sohrab, S.H. and Williams, F.A., "Extinction of Diffusion Flames Adjacent to Flat Surfaces of Burning Polymers," Journal of Polymer Science, Polymer Chemistry Edition, Vol. 19, No. 11, Nov. 1981, pp. 2955-2976.
9. Patankar, S.V., Numerical Heat Transfer and Fluid Flow, Hemisphere, Washington, D.C., 1980.
10. Chen, C.H. and T'ien, J.S., "Fire Plume Along Vertical Surfaces: Effect of Finite-Rate Chemical Kinetics," Journal of Heat Transfer, Vol. 106, No. 4, Nov. 1984, pp. 713-720.
11. Hirano, T. and Kinoshita, M., "Gas Velocity and Temperature Profiles of a Diffusion Flame Stabilized in the Stream over Liquid Fuel," Fifteenth Symposium (International) on Combustion, The Combustion Institute, Pittsburgh, 1975, pp. 379-397.
12. Lee, S.T. and T'ien, J.S., "A Numerical Analysis of Flame Flashback in a Premixed Laminar System," Combustion and Flame, Vol. 48, No. 3, Dec. 1982, pp. 273-285.
13. Mao, C.P., Kodama, H. and Fernandex-Pello, A.C., "Convective Structure of a Diffusion Flame over a Flat Combustible Surface," Combustion and Flame, Vol. 57, No. 2, Aug. 1984, pp. 209-236.

TABLE I. - NONDIMENSIONAL PARAMETERS

| Symbol         | Parameter group  | Value                  |
|----------------|--|------------------------|
| Pr             | $\bar{\nu}/\bar{\alpha}$                                 | 1                      |
| Le             | $\bar{\alpha}/\bar{D}$                                   | 1                      |
| r              | $T^*/T_\infty$   | 4.33                   |
| $Y_{O_\infty}$ | -----  | 0.231                  |
| f              | -----  | 4.0                    |
| Q              | $\bar{Q}/\bar{c}_p T_\infty$                             | 116.8                  |
| L              | $\bar{L}/\bar{c}_p T_\infty$                             | 4.33                   |
| E              | $\bar{E}/RT_\infty$                                      | 54.20                  |
| Da             | $(k^*/\bar{c}_p u_\infty^2)\bar{B}$                      | variable               |
| As             | $\bar{A}s/\rho^*$  | $2.05 \times 10^5$     |
| Es             | $\bar{E}s/RT_\infty$                                     | 50.40                  |
| S              | $\epsilon \sigma T_\infty^3 / \rho^* \bar{c}_p u_\infty$ | variable               |
|                |  | 0, no radiation        |
| $\epsilon$     | -----  | 1, blackbody radiation |

TABLE II. - PARAMETRIC STUDIES

| Case | $\bar{u}_\infty$ ,<br>(cm/s) | Da                 | S                |
|------|------------------------------|--------------------|------------------|
| 1s   | 20                           | $2.81 \times 10^6$ | 0.02091          |
| 2s   | 10                           | $1.13 \times 10^7$ | 0.04182          |
| 3s   | 5                            | $4.50 \times 10^7$ | 0.08364          |
| 4s   | 4                            | $7.03 \times 10^7$ | 0.10455          |
| 5s   | 3.33                         | $1.01 \times 10^8$ | 0.12546          |
| 6s   | 2.50                         | $1.80 \times 10^8$ | 0.16728          |
| 7s   | 1.67                         | $4.05 \times 10^8$ | 0.25092          |
| 8s   | 1.25                         | $7.20 \times 10^8$ | 0.33456 (quench) |



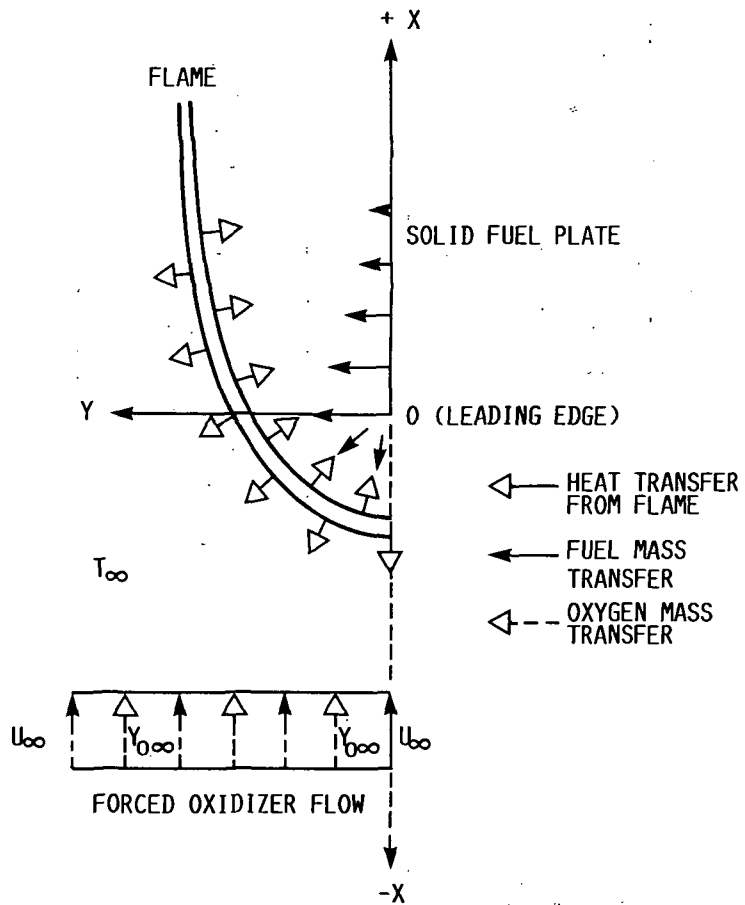


FIGURE 1.- SCHEMATIC CONFIGURATION OF THE STABILIZATION ZONE FOR AN ENVELOPE DIFFUSION FLAME (ADOPTED FROM REF. 1).

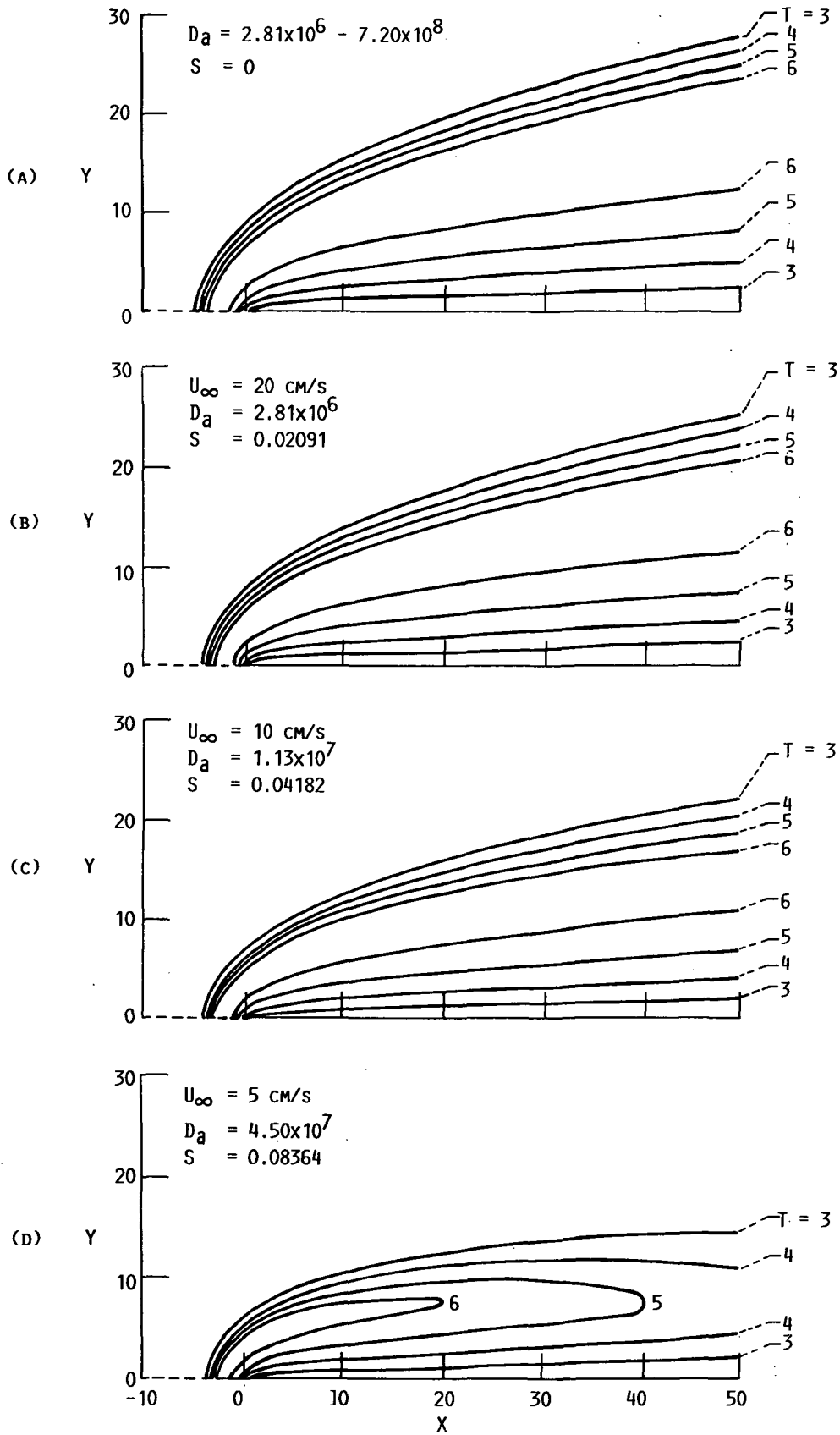


FIGURE 2.- SERIES OF TEMPERATURE CONTOUR DISTRIBUTIONS (CASE 1s - CASE 7s).

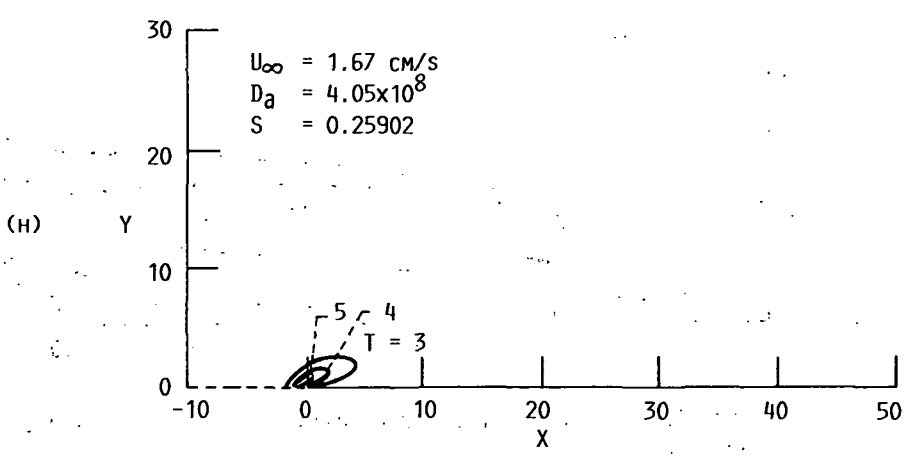
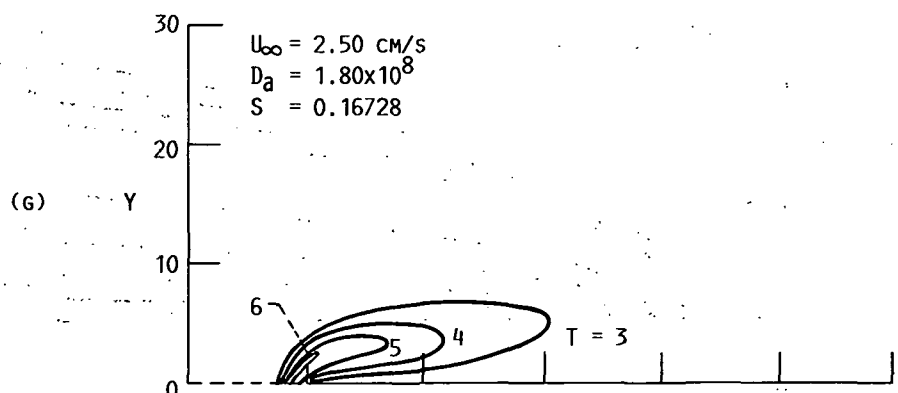
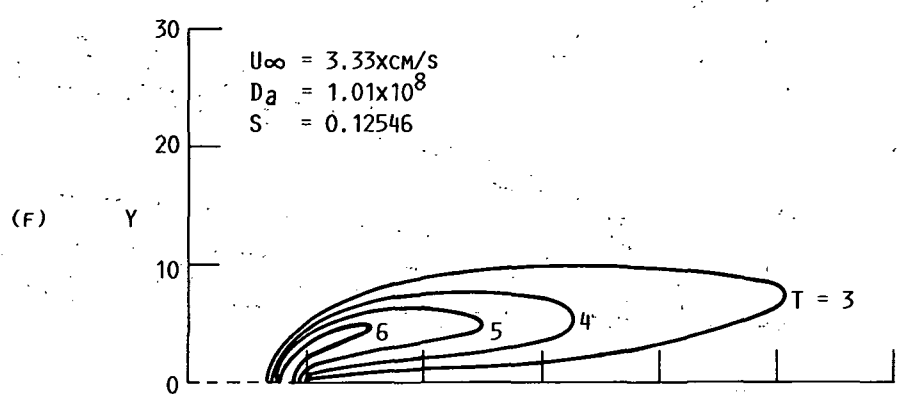
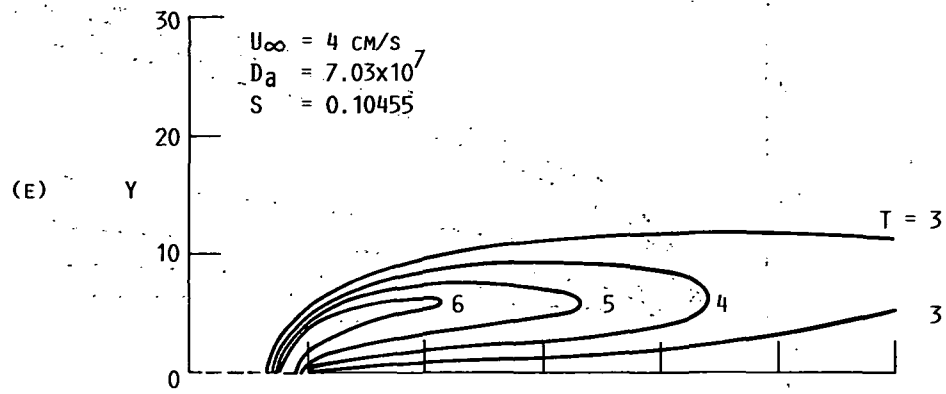


FIGURE 2.- CONCLUDED.

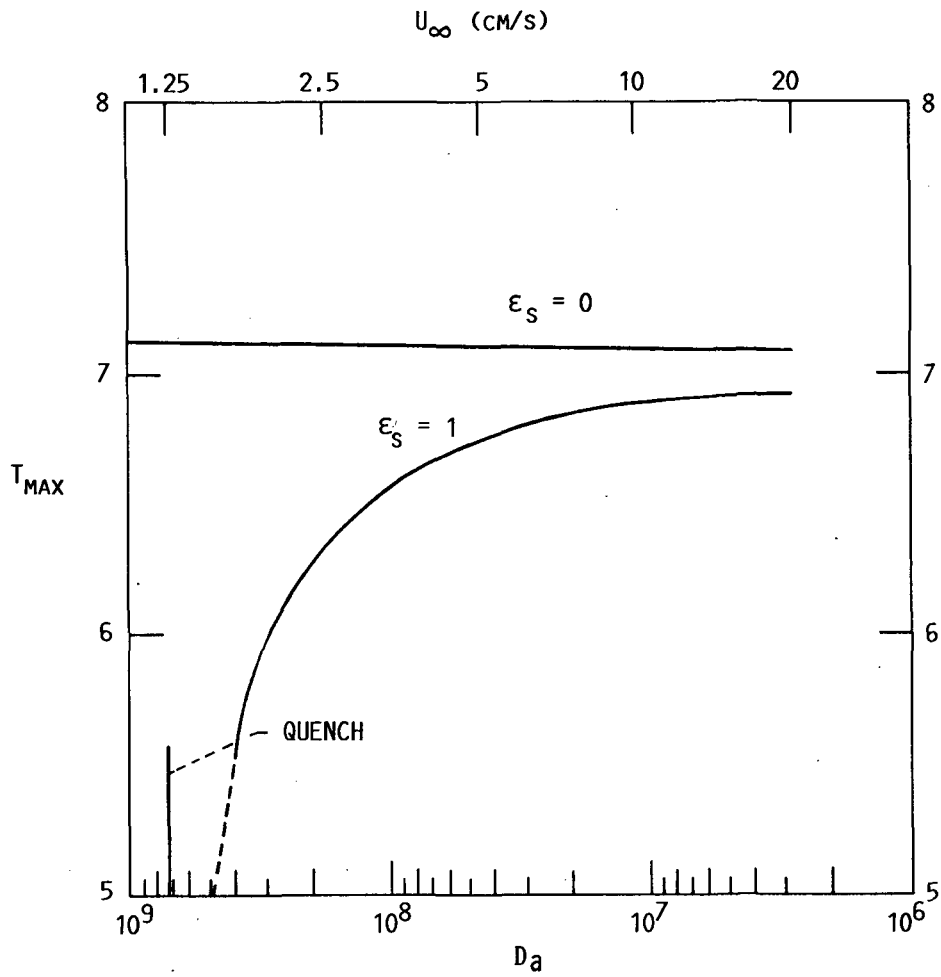


FIGURE 3.- MAXIMUM FLAME TEMPERATURE ( $T_{MAX}$ ) VERSUS DAMKOHLER NUMBER ( $D_a$ ).

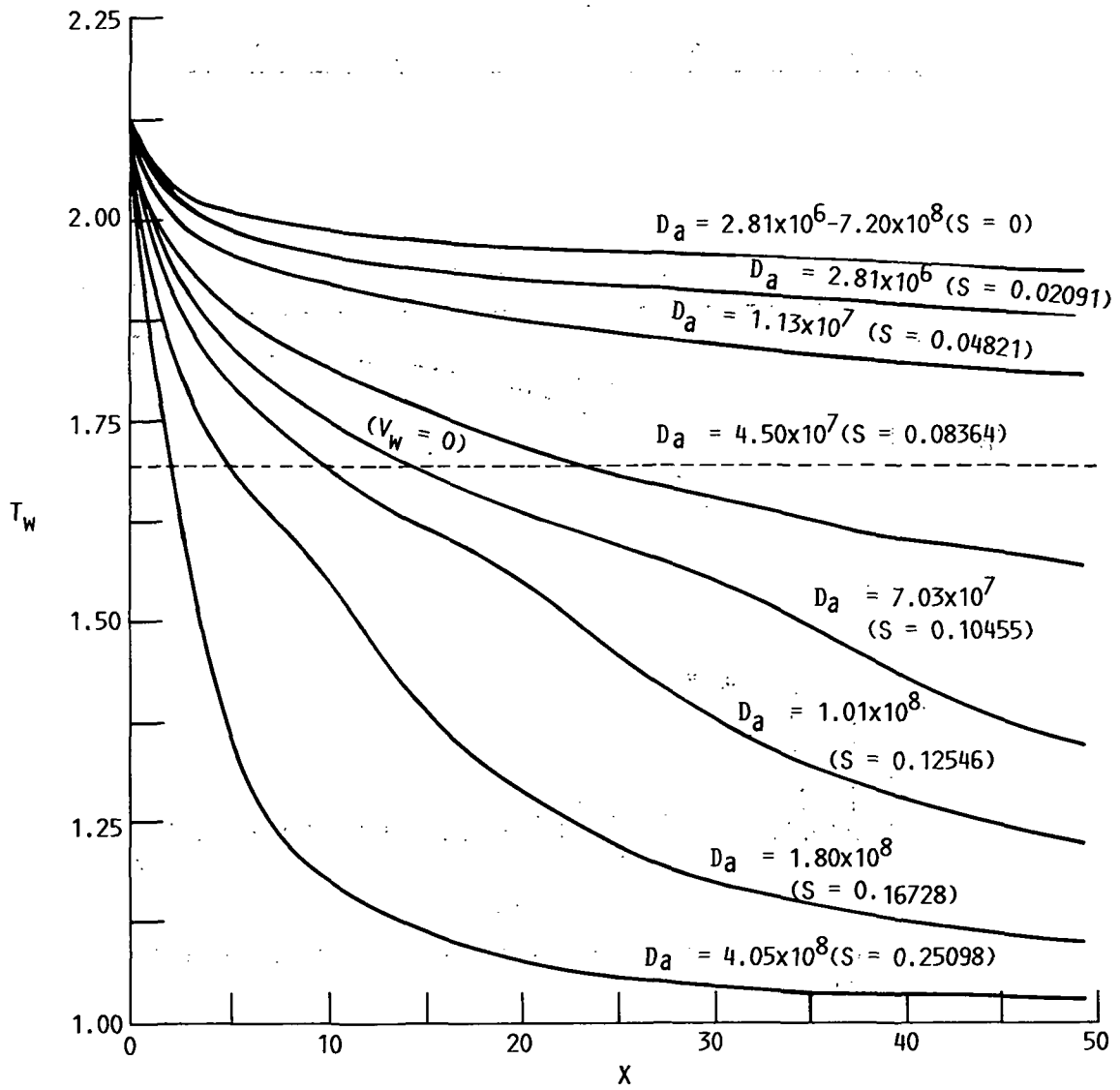


FIGURE 4.- TEMPERATURE DISTRIBUTIONS ALONG THE FUEL SURFACE (CASE 1s - CASE 7s).

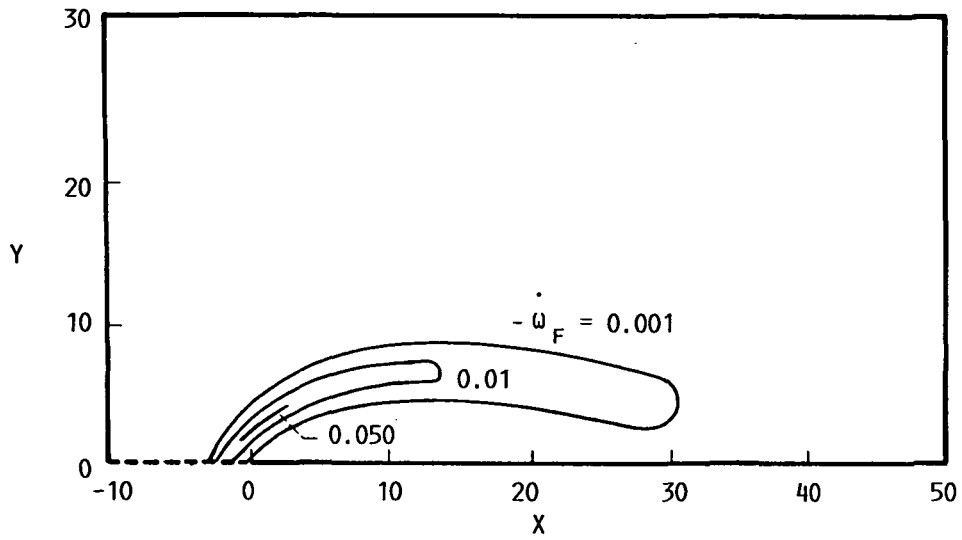


FIGURE 5.- NONDIMENSIONAL FUEL REACTIVITY CONTOURS (CASE 4s).

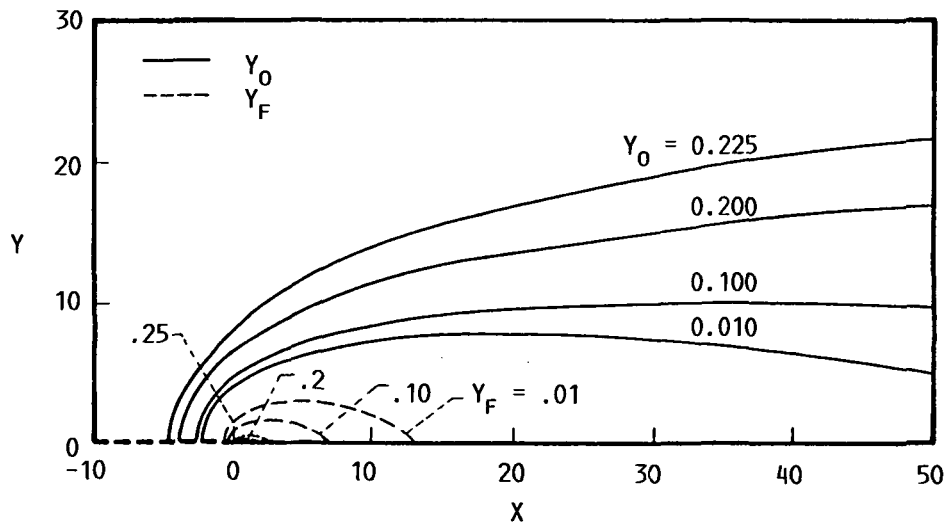


FIGURE 6.- FUEL AND OXIDIZER MASS FRACTION CONTOURS (CASE 4s).

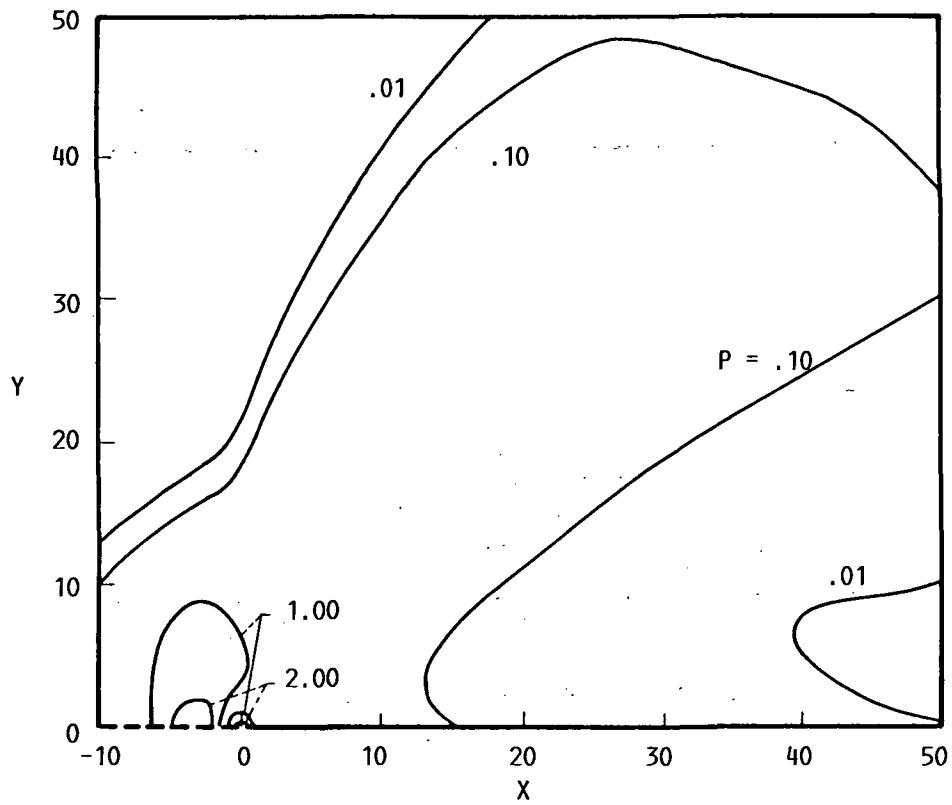


FIGURE 7.- RELATIVE ISOBAR CONTOURS (CASE 4s).

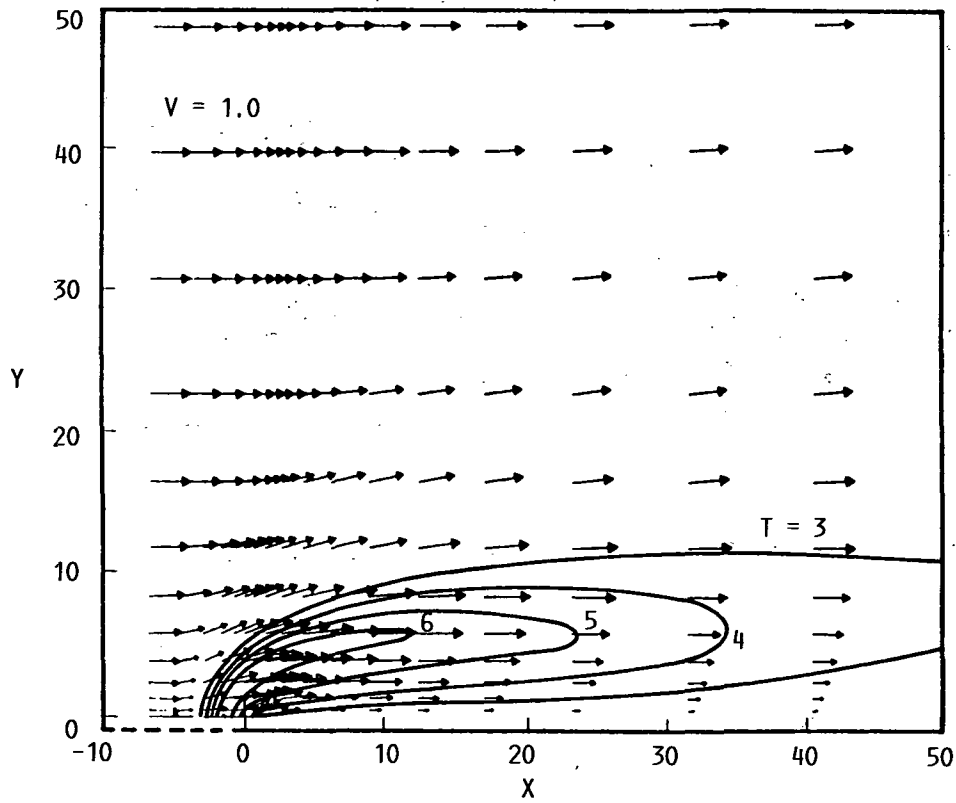


FIGURE 8.- VELOCITY VECTOR FIELD (CASE 4s).

|  |                                      |   |            |
|--|--------------------------------------|---|------------|
| 1. Report No.  | 2. Government Accession No.          | 3. Recipient's Catalog No.  |            |
| 4. Title and Subtitle<br><br>Diffusion Flame Extinction In Slow Convective Flow Under Microgravity Environment |                                      | 5. Report Date  |            |
|  |                                      | 6. Performing Organization Code<br><br>674-22-05  |            |
| 7. Author(s)<br><br>C. Chen  |                                      | 8. Performing Organization Report No.   |            |
|  |                                      | 10. Work Unit No.   |            |
| 9. Performing Organization Name and Address  |                                      | 11. Contract or Grant No.   |            |
|  |                                      | 13. Type of Report and Period Covered   |            |
| 12. Sponsoring Agency Name and Address   |                                      | 14. Sponsoring Agency Code  |            |
|  |                                      | 15. Supplementary Notes<br><br>To be presented at the Microgravity Fluid Mechanics Symposium, to be held in San Francisco, California, November 30-December 5, 1986 |            |
| 16. Abstract<br><br>See Attached   |                                      |   |            |
| 17. Key Words (Suggested by Author(s))   |                                      | 18. Distribution Statement<br><br>General Release   |            |
| 19. Security Classif. (of this report)   | 20. Security Classif. (of this page) | 21. No. of pages  | 22. Price* |



|  |  |   |  |  |            |
|--|--|---|--|--|------------|
| 1. Report No.<br><b>NASA TM-88799</b>  |  | 2. Government Accession No.                                 |  | 3. Recipient's Catalog No.   |            |
| 4. Title and Subtitle<br><b>Diffusion Flame Extinction in Slow Convective Flow Under Microgravity Environment</b>  |  |   |  | 5. Report Date   |            |
|  |  |   |  | 6. Performing Organization Code<br><b>674-22-05</b>                  |            |
| 7. Author(s)<br><b>Chiun-Hsun Chen</b>   |  |   |  | 8. Performing Organization Report No.<br><b>E-3137</b>               |            |
|  |  |   |  | 10. Work Unit No.  |            |
| 9. Performing Organization Name and Address<br><b>National Aeronautics and Space Administration<br/>Lewis Research Center<br/>Cleveland, Ohio 44135</b><br><i>ND 315753</i>  |  |   |  | 11. Contract or Grant No.  |            |
|  |  |   |  | 13. Type of Report and Period Covered<br><b>Technical Memorandum</b> |            |
| 12. Sponsoring Agency Name and Address<br><b>National Aeronautics and Space Administration<br/>Washington, D.C. 20546</b>  |  |   |  | 14. Sponsoring Agency Code   |            |
|  |  |   |  |  |            |
| 15. Supplementary Notes<br><b>Prepared for the Microgravity Fluid Mechanics Symposium, sponsored by the American Society of Mechanical Engineers, Anaheim, California, December 10-11, 1986. Chiun-Hsun Chen, National Research Council - NASA Research Associate.</b>   |  |   |  |  |            |
| 16. Abstract<br><b>A theoretical analysis is presented to study the extinction characteristics of a diffusion flame near the leading edge of a thin fuel plate in slow, forced convective flows in a microgravity environment. The mathematical model includes two-dimensional Navier-Stokes momentum, energy and species equations with one-step overall chemical reaction using second-order finite rate Arrhenius kinetics. Radiant heat loss on the fuel plate is applied in the model as it is the dominant mechanism for flame extinguishment in the small convective flow regime. A parametric study based on the variation of convective flow velocity, which varies the Damkohler number (Da), and the surface radiant heat loss parameter (S) simultaneously, is given. An extinction limit is found in the regime of slow convective flow when the rate of radiant heat loss from fuel surface outweighs the rate of heat generation due to combustion. The transition from existent envelope flame to extinguishment consists of gradual flame contraction in the opposed flow direction together with flame temperature reduction as the convective flow velocity decreases continuously until the extinction limit is reached. A case of flame structure subjected to surface radiant heat loss is also presented and discussed.</b> |  |   |  |  |            |
| 17. Key Words (Suggested by Author(s))<br><b>Microgravity combustion<br/>Diffusion flame extinction<br/>Radiation</b>  |  |   | 18. Distribution Statement<br><b>Unclassified - unlimited<br/>STAR Category 34</b> |  |            |
| 19. Security Classif. (of this report)<br><b>Unclassified</b>  |  | 20. Security Classif. (of this page)<br><b>Unclassified</b> |  | 21. No. of pages   | 22. Price* |

National Aeronautics and  
Space Administration

**Lewis Research Center**  
Cleveland, Ohio 44135

Official Business  
Penalty for Private Use \$300

**SECOND CLASS MAIL**

**ADDRESS CORRECTION REQUESTED**



Postage and Fees Paid  
National Aeronautics and  
Space Administration  
NASA-451

**NASA**

---